Proceedings of the 16th International Conference on Soil Mechanics and Geotechnical Engineering

doi:10.3233/978-1-61499-656-9-2685

Critical seismic coefficient using limit analysis and finite elements

Coefficient sismique critique en utilisant l'analyse de limite et les éléments finis

D. Loukidis
School of Civil Engineering, Purdue University, IN, USA
P. Bandini
Department of Civil Engineering, New Mexico State University, NM, USA
R. Salgado
School of Civil Engineering, Purdue University, IN, USA

ABSTRACT

Numerical limit analysis is used to determine rigorous lower and upper bounds to the horizontal critical pseudo-static seismic coefficient k_c required to cause collapse of two-dimensional slopes. Optimal bounding values of k_c are calculated by applying linear programming techniques. Additionally, conventional displacement finite element analyses were performed for selected cases using the program ABAQUS. The values of k_c and the slip surfaces obtained from the displacement finite element analyses and numerical limit analysis are in good agreement with those from both limit equilibrium methods and log-spiral upper bound method. A small number of finite element analyses using a non-associated flow rule showed that soil dilatancy influences the value of k_c, and that limit analysis and limit equilibrium solutions may be slightly unconservative.

RÉSUMÉ

L'analyse de limite numérique est employée pour déterminer les limites inférieures et supérieures rigoureuses au coefficient sismique pseudo-statique critique horizontal k_c nécessaries pour causer l' effondrement des talus bidimensionnelles. Nous avons calculé des limites optimales du k_c en appliquant des techniques de programmation linéaire. De plus, nous avons fait des analyses d'élément fini dans certains cas choisis en utilisant le programme ABAQUS. Les valeurs du k_c et les surfaces de glissement provenant des analyses d'élément fini de déplacement et des analyses de limite supérieure numérique correspondent bien à ceux obtenues avec les méthodes d'équilibre limite et le méthode de limite supérieure logspiral. Un nombre restreint de analyses d'élément fini en utilisant une règle d'écoulement non-associée a prouvé que la dilatance de sol influence la valeur du k_c, et que l'analyse limite et les solutions d'équilibre limite peuvent être légèrement non conservatives.

1 INTRODUCTION

The pseudostatic approach is commonly used in engineering practice for the design of slopes in seismic areas. The seismic safety of a slope can be expressed by a single parameter, the critical seismic coefficient k_c, as an alternative to the safety factor (Sarma, 1973). The critical seismic coefficient k_c is defined as the ratio of the seismic acceleration a_c to the acceleration of gravity g (= 9.81 m/s^2) that yields a factor of safety equal to unity. Moreover, the critical seismic coefficient k_c is one of the most important parameters entering the calculations for the sliding block method proposed by Newmark (1965), widely used in the estimation of earthquake-induced, permanent displacements in earth structures.

Although more elaborate analyses are nowadays available, such as non-linear FEM, the limit equilibrium (LE) method is still extensively employed to perform pseudostatic slope stability calculations. A number of different LE schemes have been formulated for the direct determination of the critical seismic coefficient k_c, without the need for iterations or for the calculation of the factor of safety (Sarma, 1973; Spencer, 1978; Sarma, 1979; Kim & Sitar, 2004). However, LE method solutions satisfy only the global equilibrium of the failing soil mass. Equilibrium inside the failing mass and strain compatibility are not checked. Thus, results yielded by the limit equilibrium method are only approximations to the true collapse load. Limit analysis is a powerful mathematical tool that provides rigorous lower and upper bounds to the exact collapse load, as long as it is assumed that the soil follows an associated flow rule. Thus, limit analysis can be used to check the validity of limit equilibrium solutions.

Past research efforts have shown that results from limit equilibrium methods are in good agreement with limit analysis bounds for the static slope stability problem (Yu et al., 1998; Kim et al., 2002). In this paper, numerical limit analysis is applied to the problem of two-dimensional pseudostatic slope stability. Results in terms of k_c and critical slip surface are compared with those obtained from limit equilibrium methods. Finite element simulations were also carried out for some of the investigated cases. Throughout the present study, the soil was assumed to follow the Mohr-Coulomb failure criterion. Since an associated flow rule is not an accurate representation of the real soil behavior, a limited number of finite element analyses were used to assess the impact of non-associativity on the pseudostatic slope stability problem.

2 METHODS OF ANALYSIS

2.1 *Numerical limit analysis*

Linear programming techniques combined with finite element discretiazation were used to obtain optimal statically admissible stress fields and kinematically admissible velocity (or strain rate) fields, from which the lower and upper bounds are derived, respectively. The lower and upper bound formulations of Sloan (1988) and Sloan and Kleeman (1995), later modified by Kim et al. (2002) to account for porewater pressures and complex soil profiles, were extended to compute the critical seismic coefficient (Loukidis et al., 2003). Bounds calculated using this limit analysis approach are referred herein as numerical lower and upper bounds. Although the current formulation is capable of calculating either the vertical or the horizontal critical seismic coefficients, computations performed herein consider only a horizontal k_c.

For the lower bound analysis, we seek a statically admissible and safe stress field that yields the highest possible value of k_c, with the soil mass being discretized into three-noded triangular elements in which the stresses vary linearly. For the upper bound analysis, we seek a kinematically admissible velocity field at the state of collapse that yields the lowest highest possible value of k_c, with the soil being divided into three-noded triangular elements in which the velocities vary linearly (constant strains). Differently from traditional displacement-based finite elements, each node of the finite element mesh in numerical limit analysis is unique to a given element. This mesh characteristic allows for statically admissible stress discontinuities and kinematically admissible velocity discontinuities of zero thickness. Extension elements are incorporated into the lower bound mesh to extend the stress field to the infinite half space (Sloan 1988). The total unit weight γ, the internal friction angle ϕ, and the cohesion c of the soil are assumed to be constant within an element. For complete description of the formulation of the lower and upper bound problems using linear programming, the reader is referred to Sloan (1988), Sloan and Kleeman (1995), Loukidis et al. (2003) and Bandini (2003). Fig. 1 shows the sign and notation adopted in this study. At the collapse state, $k_h = k_c$.

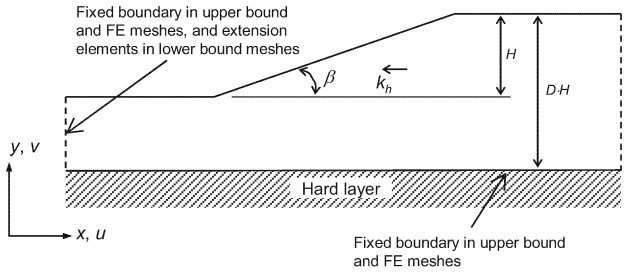

Figure 1. Schematic of problem configuration for simple homogeneous slopes.

2.2 *Displacement finite element analysis*

The finite element method has traditionally been used in geotechnical engineering to obtain good approximations of collapse loads. However, a careful discretization in the vicinity of the anticipated shear band is required for an accurate FE. Unstructured meshes composed of six-noded, plane-strain triangular elements were used to discretize the soil mass in this study. Boundary conditions are shown in Fig. 1. The finite element mesh was extended laterally to the point at which the left and right boundaries did not have any effect on the collapse mechanism. A soil constitutive model following the Mohr-Coulomb failure criterion was assigned to the soil for direct correspondence with limit analysis. The value of k_c is obtained once the analysis reaches the collapse state. At the collapse state, the shear band, defined herein based on plastic shear strains, extends across the entire height of the slope, and the inclination of the crest displacement vs. applied body load curve tends to infinity.

2.3 *Log-spiral upper bound and Limit equilibrium*

The upper bound method by Chang et al. (1984) provides a rigorous upper bound to the critical seismic coefficient k_c for a homogeneous slope by establishing a kinematically admissible failure mechanism along a log-spiral slip surface. In this study, the log-spiral is assumed to pass through the toe of the slope. For more general cases, porewater pressures can be also incorporated into the formulation (Loukidis et al., 2003).

Three limit equilibrium methods were employed to estimate the critical seismic coefficient k_c: Bishop's simplified (Bishop, 1955), Sarma's method (Sarma, 1973) and Spencer's method (Spencer, 1978). These differ from each other mainly on the assumptions made regarding the interslice forces. For the purpose of this study, the program PCSTABL (PCSTABL6, Purdue University) was modified to yield directly the minimum k_c instead of the static factor of safety using the above methods. For Spencer's method, it was assumed that the inclination angle of the interslice forces with respect to the horizontal is constant throughout the slope.

3 RESULTS

Results from numerical limit analysis for homogeneous slopes with inclination $\beta = 20^o$, 30^o, and 45^o are presented in Fig. 2. The ratio D of the vertical distance between the crest and the hard layer to the height of the slope H (Fig. 1) was set equal to 1.5. An effective way to produce normalized plots is to use the parameter λ (Leshchinsky and San, 1994; Michalowski, 2002):

$$\lambda = \frac{c}{\gamma \cdot H \cdot \tan\phi} \tag{1}$$

where γ = soil unit weight; and H = slope height. The friction angle ϕ of the soil was varied from 10^o to 40^o, and no vertical seismic loading was considered. Although calculations were actually performed using $\gamma = 20\text{kN/m}^3$ and $H = 20\text{m}$, this is not relevant as the charts in Fig. 2 are normalized by these two parameters. The number of elements in meshes used in numerical limit analysis ranged from 1670 to 1813 for the lower bound and 2303 and 2550 for the upper bound.

In addition, log-spiral upper bounds and results from Spencer's limit equilibrium method are plotted in Fig. 2. The difference between the numerical lower and upper bounds increases with both the friction angle and the slope angle, and show an average difference of ±4, 6, and 10% for $\beta = 20^o$, 30^o, and 45^o, respectively, with respect to their mean values.

The log-spiral upper bound values are considerably lower (better) than those from the numerical upper bound analysis. This is because, for the case of homogeneous slopes, the log-spiral mechanism is indeed very close to the exact collapse mechanism. Moreover, in the log-spiral upper bound approach, all the plastic dissipation takes place on an infinitely thin discontinuity. Although refining the mesh in the high plasticity region in the numerical limit analysis improves the value of the upper bound, the plastic strain rates are still localized in a region of finite width. Considering the log-spiral upper bound instead of the numerical upper bound reduces the difference between the bounds with respect to their mean to ± 2, 3, and 3% for $\beta = 20^o$, 30^o, and 45^o, respectively, for the considered range of λ. Thus, the true k_c value for simple homogeneous slopes is defined almost exactly by the log-spiral upper bound and the numerical lower bound, from a practical point of view.

The k_c values obtained from Spencer's method using the irregular random surface generator nearly coincide with the log-spiral upper bound for most cases, as shown in Fig. 2. Results from Bishop's simplified method lie between the numerical lower and upper bounds for almost all the cases studied. Bishop's simplified method shows a tendency to produce results marginally more conservative than those of Spencer's method for the higher ϕ values. For $\phi \leq 25^o$, this tendency reverses.

As λ increases and ϕ decreases, the failure mechanism penetrates deeper into the soil profile. For large λ values, the failure mechanism tends to develop tangent to the hard layer and extend laterally to extremely large distances from the slope. For these cases, Spencer's method computations were performed using the block option available in PCSTABL rather than the irregular surface generator, in order to reproduce slip surfaces that were mostly tangent to the hard layer. These cases, referred herein as singularity cases, are denoted in Fig. 2 by

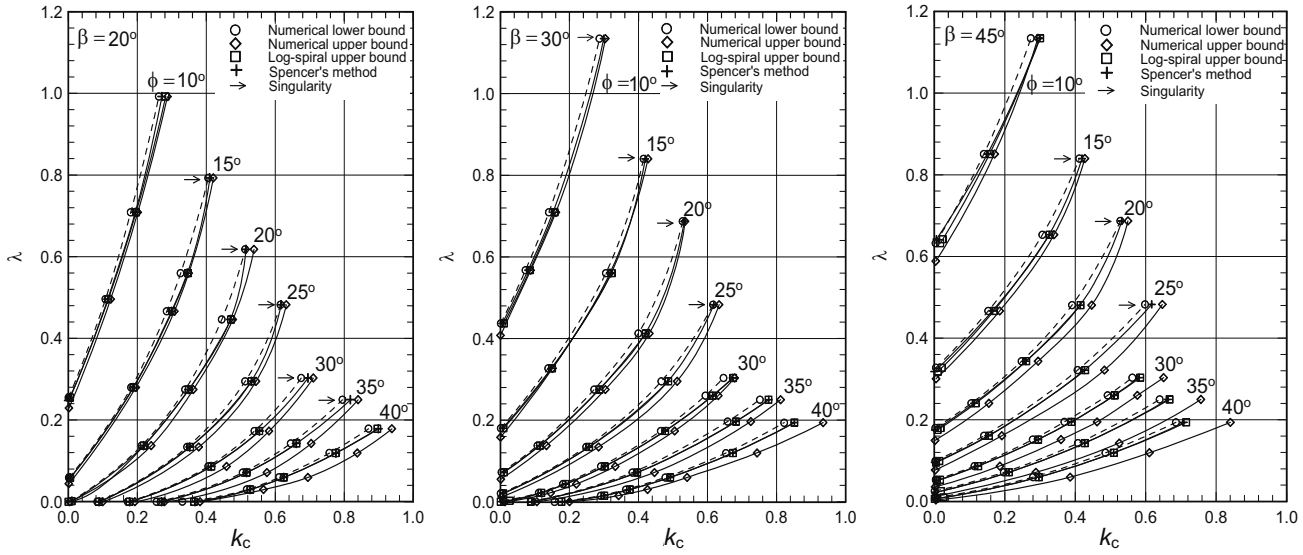

Figure 2. Horizontal critical seismic coefficient k_c as function of λ and friction angle ϕ.

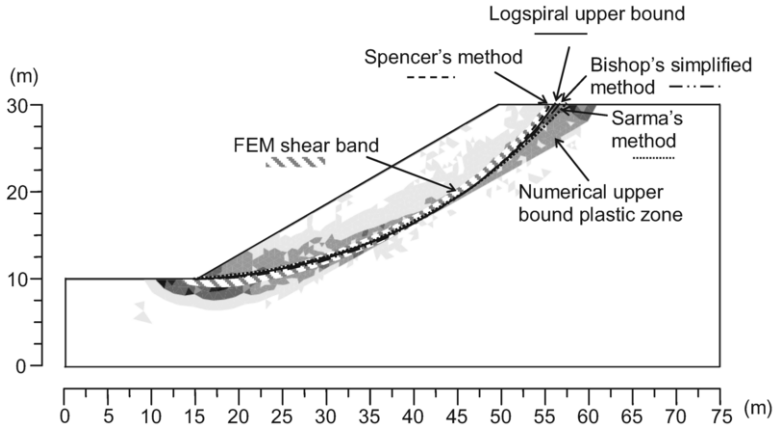

Figure 3. Comparison of critical slip surfaces obtained from limit equilibrium methods and plasticity zones determined from numerical upper bound analysis and the finite element method.

horizontal arrows. For more discussion on these special cases, the reader is referred to Loukidis et al. (2003).

Fig. 3 shows a comparison of the critical slip surfaces predicted by the limit equilibrium methods and the log-spiral upper bound, the shear band obtained from the finite element analysis, and the plasticity zone from the numerical upper bound analysis, for the case of $\beta = 30^o$, c = 20kPa, and $\phi = 30^o$. It can be seen that the failure mechanisms predicted by all the methods employed are in excellent agreement.

Resulting values of k_c for selected cases with $\beta = 30^o$ are presented in Table 1. Displacement finite element analysis and the Sarma (1973) limit equilibrium method computations were also performed for these cases. The commercial program ABAQUS (Hibbit et al., 2001) was used for the FEM analyses. The dilatancy angle in FEM analyses was set equal to the friction angle to allow direct comparisons with the results from limit analysis. Generally, the finite element predictions fall below the log-spiral upper bound, but in some cases, finite element analysis does not yield values of k_c within the narrow range defined by the numerical lower and the log-spiral upper bounds. This is most likely due to insufficient mesh refinement, although the element size in the vicinity of the shear band was set to be only 2% of the slope height.

Table 1. Comparison of the horizontal critical seismic coefficient k_c for $\beta = 30^o$

ϕ (deg)	20	20	20	30	30	30	30	30
λ	0.137	0.275	0.412	0.022	0.043	0.087	0.173	0.260
Numerical lower bound	0.107	0.271	0.399	0.111	0.181	0.291	0.464	0.593
Numerical upper bound	0.133	0.304	0.431	0.145	0.220	0.331	0.504	0.631
Log-spiral upper bound	0.114	0.287	0.420	0.118	0.189	0.302	0.477	0.615
Finite elements	0.114	0.285	0.415	0.118	0.190	0.304	0.478	0.613
Spencer's method	0.113	0.286	0.420	0.117	0.188	0.302	0.477	0.615
Bishop's simplified	0.114	0.284	0.416	0.118	0.188	0.298	0.469	0.603
Sarma's method	0.109	0.279	0.414	0.116	0.185	0.295	0.469	0.607

4 EFFECT OF NON-ASSOCIATED FLOW RULE

Numerical simulations of static slope stability by Zienkiewicz et al., (1975) and Manzari and Nour, (2000) suggest that non-associated flow rule leads to smaller values of collapse loads. In the case of a non-associated flow rule, the lower and upper bound theorems no longer hold. Drescher and Detournay (1993) formulated an upper bound analysis that accounts for non-associativity, in which the true strength parameters are substituted by a set of modified strength parameters proposed by Davis (1968). However, it is well known that upper bounds yielded by this approach are still non-rigorous. To date, finite element analysis is the only way to obtain reliable estimates of collapse loads in the case of a non-associated flow rule. Finite element analysis using ABAQUS were performed for the cases of $\beta = 30^o$, $\lambda = 0.087$ and $\phi = 30^o$ and $\beta = 45^o$, $\lambda = 0.06$ and $\phi = 40^o$. From Fig. 4 it can be seen that the difference between the collapse load for the associative case ($\phi = \psi$) and those corresponding to $\phi - \psi = 25^o$ is around 15%. The difference in the k_c value appears to become greater with ϕ.

It is interesting to note that although limit equilibrium methods do not make any consideration regarding the dilatancy angle of the soil, their results are always consistent with the solution of the problem with $\phi = \psi$. Since for real soil it is true that $\phi - \psi > 25^o$, the FE analyses presented herein suggest that the k_c yielded by the limit equilibrium methods routinely used in practice may be slightly unconservative.

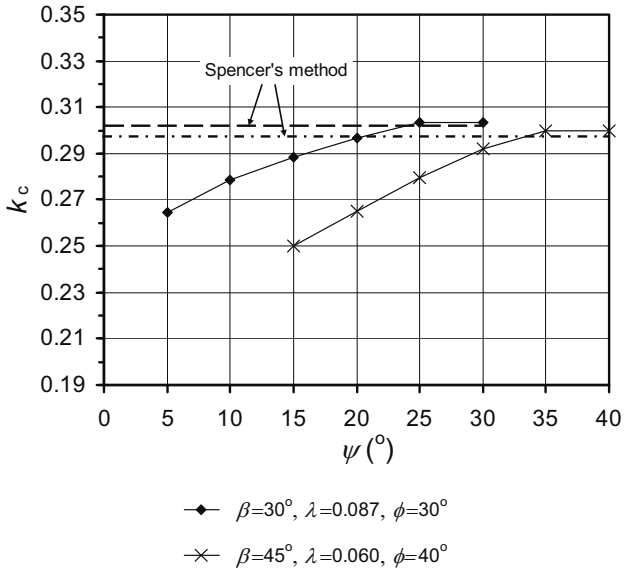

Figure 4. Effect of the dilatancy angle ψ on the value of k_c.

5 SUMMARY AND CONCLUSIONS

The problem of seismically loaded soil slopes was studied using numerical limit analysis and displacement-based finite element analysis. Results were compared with those generated by limit equilibrium and the log-spiral upper bound method. The following conclusions are drawn:

1) For homogeneous slopes, the numerical lower bound and the log-spiral upper bound form a very narrow band, thus, defining the true value of k_c.
2) The results of the critical seismic coefficient from all three limit equilibrium methods used in this study are in good agreement with the rigorous bounds calculated with limit analysis. Moreover, limit equilibrium methods are capable of closely predicting the shape and location of the failure surface.
3) Displacement finite element analyses using a non-associated flow rule indicate that soil dilatancy influences the value of k_c to a certain extent. Thus, limit equilibrium solutions used in practice may be slightly unconservative.

ACKNOWLEDGMENT

The limit analysis results were produced using modified versions of the codes LOWER and UPPER written by Professor S. W. Sloan (University of Newcastle, Australia). The authors thank Professor Sloan for making the original codes available to them.

REFERENCES

Bandini, P. (2003). *Numerical limit analysis for slope stability and bearing capacity calculations.* Ph.D. Thesis, Purdue University, West Lafayette, IN, U.S.A.

Bishop, A.W. (1955). The use of the slip circle in the stability analysis of slopes. *Géotechnique*, Vol. 5, No. 1, pp. 7–17.

Chang, C-J., Chen, E.F., and Yao, J.T.P. (1984). Seismic displacements in slopes by limit analysis. *J. Geotech. Engrg*, ASCE, Vol. 110, No. 7, pp. 860–874.

Davis, E.H. (1968). Theories of plasticity and the failure of soil masses. In Soil *Mechanics: Selected Topics*, (ed. I. K. Lee), London: Butterworth, pp. 341–380.

Drescher, A. and Detournay, E. (1993). Limit load in translational failure mechanisms for associative and non-associative materials. *Géotechnique*, Vol. 43, No. 3, pp. 443–456.

Hibbitt, H.D., Karlsson, B.I. and Sorensen, P. (2001). *ABAQUS/Standard User's Manual - Version 6.2.* Hibbitt, Karlsson & Sorensen, Inc., Pawtucket, RI, USA.

Kim, J.M., Salgado, R. and Lee, J. (2002) Stability analysis of complex soil slopes using limit analysis. *J. Geotech. and Geoenvir. Engrg.*, ASCE, Vol. 128, No. 7, pp. 546–557.

Kim, J. and Sitar, N. (2004). Direct estimation of Yield Acceleration in Slope Stability Analyses. *J. Geotech. and Geoenvir. Engrg.*, ASCE, Vol. 130, No. 1, pp. 111–115.

Leshchinsky, D. and San, K-C. (1994). Pseudostatic Seismic Stability of Slopes: Design Charts. *J. Geotech. Engrg*, ASCE, Vol. 120, No. 9, pp. 1514–1532.

Loukidis, D., Bandini, P. and Salgado, R. (2003). Stability of seismically loaded slopes using limit analysis. *Géotechnique*, Vol. 53, No. 5, pp. 463–479.

Manzari, M. T. & Nour, M. A. (2000). Significance of soil dilatancy in slope stability analysis. *J. Geotech. and Geoenvir. Engrg.*, ASCE, Vol. 126, No. 1, pp. 75-80.

Michalowski, R. L. (2002). Stability Charts for Uniform Slopes. *J. Geotech. and Geoenvir. Engrg.*, ASCE, Vol. 128, No. 4, pp. 351–355.

Newmark, N. M. (1965). Effects of earthquakes on dams and embankments. Fifth Rankine Lecture, *Géotechnique*, Vol. 15, No. 2, pp.139-159.

PCSTABL6: Users's Manual, School of Civil Engineering, Purdue University, West Lafayette, Ind., USA, 1999.

Sarma, S.K. (1973). Stability analysis of embankments and slopes. *Géotechnique*, Vol. 23, No. 3, pp. 423–433.

Sarma. S. K. (1979). Stability analysis of embankments and slopes. *J. Geotech. Engrg. Div.*, ASCE, Vol. 105, No. GT12, 1511-1524.

Sloan, S.W. (1988). Lower bound limit analysis using finite elements and linear programming, *Int. J. Numerical and Analytical Methods in Geomech.*, Vol. 12, pp. 61–77.

Sloan, S.W. and Kleeman, P.W. (1995). Upper bound limit analysis using discontinuous velocity fields, *Computer Methods in Applied Mech. and Engrg*, Vol. 127, pp. 293–314.

Spencer, E. (1978). Earth slopes subjected to lateral acceleration. *J. Geotech. Engrg. Div.*, ASCE, Vol. 104, No. GT12, pp. 1489–1500.

Yu, H. S., Salgado, R., Sloan, S. W., & Kim, J. M. (1998). Limit analysis versus limit equilibrium for slope stability. *J. Geotech. and Geoenvir. Engrg.*, ASCE, Vol. 124, No. 1, pp. 1-11.

Zienkiewicz, O. C., Humpherson, C., & Lewis, R. W. (1975). Associated and non-associated viscoplasticity and plasticity in soil mechanics. *Géotechnique*, Vol. 25, No. 1, pp. 671-689.